Evaluation and translation of combination therapies in oncology – A quantitative approach

European Journal of Pharmacology 834 (2018) 327–336

Contents lists available at ScienceDirect

European Journal of Pharmacology

journal homepage: www.elsevier.com/locate/ejphar

Full length article

Evaluation and translation of combination therapies in oncology – A quantitative approach

Tim Cardilin[a,b,*], Joachim Almquist[a], Mats Jirstrand[a], Johan Gabrielsson[c]

[a] Fraunhofer-Chalmers Centre, Chalmers Science Park, Gothenburg, Sweden
[b] Department of Mathematical Sciences, Chalmers University of Technology and University of Gothenburg, Gothenburg, Sweden
[c] Department of Biomedical Sciences and Veterinary Public Health, Swedish University of Agricultural Sciences, Uppsala, Sweden

ARTICLE INFO

Keywords:
Tumor static exposure
Pharmacokinetic/pharmacodynamic modeling
Dose optimization
Inter-species scaling

ABSTRACT

Quantitative techniques improve our understanding of tumor volume data for combination treatments and its translation across *in vivo* models and species. The focus of this paper is therefore on understanding *in vivo* data, highlighting key structural elements of pharmacodynamic tumor models, and challenging these methods from a translational point of view. We introduce the concept of Tumor Static Exposure (TSE) both for single and multiple combined anticancer agents. The TSE curve separates all possible exposure combinations into regions of tumor growth and tumor shrinkage. Moreover, the degree of curvature of the TSE curve indicates the degree of synergy or antagonism. We demonstrate the TSE approach by two case studies. The first examines a combination of the drugs cetuximab and cisplatin. The TSE curve associated with this combination reveals a weak synergistic effect, suggesting only modest gains from combination therapy. The second case study examines combinations of ionizing radiation and a radiosensitizing agent. In this case, the TSE curve exhibits a pronounced curvature, indicating a strong synergistic effect; tumor regression can be achieved at significantly lower exposure levels and/or radiation doses. Finally, an allometric approach to human dose prediction demonstrates the translational power of the model and the TSE concept. We conclude that the TSE approach, which embodies model-based measures of both drug (potency) and target properties (tumor growth rate), has a strong potential for ranking of compounds, supporting compound selection, and translating preclinical findings to humans.

1. Introduction

Pharmacodynamic models are commonly used to aid decision-making in drug discovery and development. In oncology, *tumor growth inhibition* models have been used extensively in the past decades (Evans et al., 2014; Ribba et al., 2014; Simeoni et al., 2004; Tate et al., 2014). For a recent review, see Mould et al. (2015). Some growth models are empirical (Simeoni et al., 2004), whereas others have a more mechanistic foundation (Jumbe et al., 2010; Wendling et al., 2016). After being calibrated to experimental data, the models are used to evaluate, predict, and guide future experimental designs (Hutchinson et al., 2016). Models are also used in translational efforts to predict first-in-man doses, using techniques such as allometric scaling (Boxenbaum, 1982, 1984).

Tumor growth inhibition models also exist for combination therapies (Goteti et al., 2010; Rocchetti et al., 2013), with the objective of evaluating and comparing different dose combinations with respect to efficacy and drug synergies. Many techniques have been proposed to evaluate drug interactions (Foucquier and Guedj, 2015). Of these, perhaps the most commonly used approach is the isobologram, which plots iso-effective dose combinations and determines synergy or antagonism based on the shape of the resulting curve (Grabovsky and Tallarida, 2004; Tallarida, 2006). Until recently, no isobologram-like techniques had been explored for different exposure-based models, including tumor models. Moreover, tumor models and techniques have been studied primarily for chemical interventions, thereby excluding an important pillar of modern oncology treatment – radiation therapy (Baskar et al., 2012).

This paper focuses on two questions: *Can quantitative techniques provide a better understanding of tumor volume data when combinations of chemicals and radiation are used?* and *What translational potential does such an approach have?* Our aim is to chisel out relevant model structures that enhance both the underlying mechanisms of action and the predictive power of the model. The methodology is demonstrated by *in vivo* data from two previous studies (Cardilin et al., 2017, 2018). Case study I introduces the Tumor Static Concentration (TSC) for both a

* Corresponding author at: Fraunhofer-Chalmers Centre, Chalmers Science Park, Gothenburg, Sweden.
E-mail addresses: tim.cardilin@fcc.chalmers.se (T. Cardilin), johan.gabrielsson@slu.se (J. Gabrielsson).

https://doi.org/10.1016/j.ejphar.2018.07.041
Received 12 June 2018; Accepted 19 July 2018
Available online 20 July 2018

single compound and multiple compounds given in combination. The analysis focuses specifically on deriving useful quantitative tools and then implementing graphical ways to view additivity, synergy or antagonism based on exposure metrics. Case study II expands the methods to also include radiation therapy as a co-variate. The combination of drug concentrations and radiation is then called Tumor Static Exposure (TSE). Case study II examines combination therapy with ionizing radiation and a radiosensitizing agent that exhibit a substantial level of synergy, manifesting as a more pronounced curvature of the TSE curve. We also thoroughly describe the two semi-mechanistic tumor models used to describe the experimental data in the case studies. Finally, we discuss how TSE can be used in translational efforts, be implemented into the drug discovery process, and for communication with a biologically-oriented audience.

2. Background

The concept of a threshold concentration has been applied to various tumor models and for different anti-cancer agents (Jumbe et al., 2010; Magni et al., 2006; Simeoni et al., 2004). Jumbe et al. (2010) derived the TSC for a single compound. Koch et al. (2009) derived an equation for threshold concentrations for a combination of two compounds. Later, the TSC curve was introduced as a graphical tool contrasting the isobologram (Cardilin et al., 2017; Gabrielsson et al., 2016). In particular, Cardilin et al. (2017) discussed how the shape of the TSC curve was associated with the combined effect (synergy or antagonism) of the combination treatment. Moreover, a TSC-like curve was also proposed by Miao et al. (2016) and for more general combination effect terms by Koch et al. (2016) under the name *half maximal-effect curve*. Most recently, Cardilin et al. (2016, 2018) extended the TSC concept to combinations involving ionizing radiation by introducing the Tumor Static Exposure (TSE) curve. In this section, we provide a brief intuitive description of the TSE concept. We refer to Appendix A for a more technical treatment of the subject.

The tumor is exposed to a single compound A during monotherapy (Fig. 1a), where C_A denotes the plasma concentration of drug. If the drug is sufficiently potent, at some concentrations maintained over an extended period of time, the tumor will start to shrink. At concentrations below the TSC, which are insufficient for tumor regression, the drug will at best slow down the tumor growth. In particular, there will also be a value of C_A in between that will keep the tumor in stasis, which we call the TSC value (Fig. 1a). In the case of radiation therapy, or when plasma concentrations cannot be measured, we may prefer to use the dose. For example, we may define a Tumor Static Dose to be the minimum daily radiation dose that will keep the tumor in stasis. This will lead to different values depending on administration schedule. In order to cover both cases we generally refer to the concept as Tumor Static Exposure (TSE).

The TSE concept can be generalized to the case where two compounds are given simultaneously as combination therapy. Let A and B denote the compounds and let C_A, and C_B be their plasma concentrations. For each fixed value of C_A, we may find a value of C_B such that maintained simultaneous exposure to both compounds leads to tumor stasis. Hence, we obtain a collection of concentration pairs (C_A, C_B) that all lead to tumor stasis. These pairs form a curve in the plane formed with C_A along the x-axis and C_B along the y-axis (Fig. 1b). We refer to this curve as the TSE curve for the compounds A and B. Note that this curve separates regions of concentration pairs corresponding to tumor growth (red) and tumor shrinkage (green).

This procedure can be extended to combinations involving three or more compounds, leading to a hypersurface in higher-dimensional concentration space. The scenario with three compounds A, B, and C with plasma concentrations C_A along the x-axis, C_B along the y-axis, and C_C along the z-axis is illustrated in Fig. 1c.

3. Case study I: cetuximab and cisplatin

3.1. Problem formulation

This case study is based on results that were reported in a previous publication (Cardilin et al., 2017). Cetuximab is an epidermal growth factor receptor (EGFR) inhibitor used clinically to treat certain colorectal and head-and-neck cancers, either as monotherapy or as combination therapy together with, *e.g.,* irinotecan, cisplatin and other platinum-based chemotherapy, or radiation (Bou-Assaly and Mukherji, 2010; Reynolds and Wagstaff, 2004). This *in vivo* study was aimed at investigating combination therapy with cetuximab and cisplatin to treat non-small cell lung cancer (NSCLC). Our goal was to develop a tumor model to describe the experimental data and use the model for evaluation with respect to synergy and overall efficacy using TSE curves.

3.2. Experimental data

Forty patient-derived xenograft (PDx) models in female mice were used in the study. The animals were divided into four treatment arms with $N = 10$ animals in each of the following arms: (A) vehicle, (B) cetuximab monotherapy (30 mg/kg per dose), (C) cisplatin monotherapy (5 mg/kg per dose), and (D) combination therapy with cetuximab (30 mg/kg per dose) and cisplatin (5 mg/kg per dose). The mice were given doses twice a week for two weeks. Tumor length (L) and width (W) were measured twice a week for 28 days. Tumor volumes were estimated using the formula: $V = L \times W^2/2$. The details of this

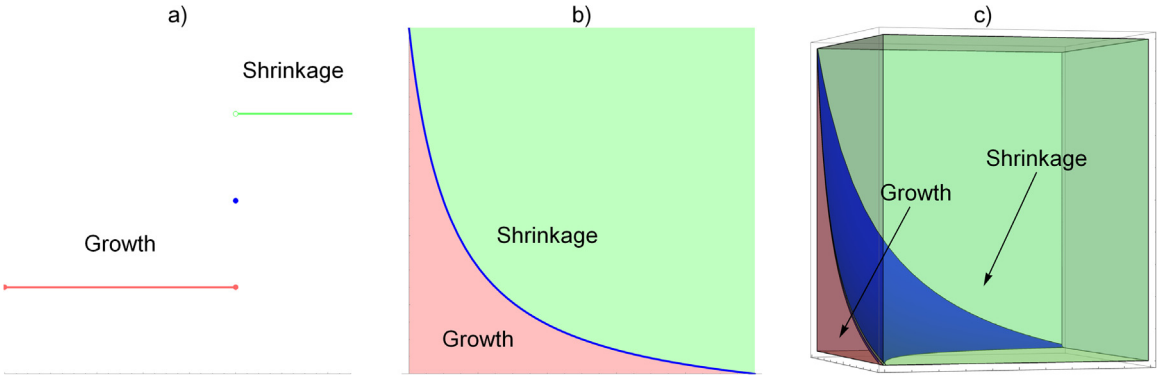

Fig. 1. a) TSE value of an anti-cancer agent (black). Exposure lower than the TSE value (red) results in tumor growth, whereas exposure greater than the TSE value (green) results in tumor shrinkage. b) TSE curve for combinations of two anti-cancer agents with concentrations C_1 and C_2. Exposure pairs below the curve (red) yield tumor regression, whereas exposure pairs above the curve (green) yields tumor shrinkage. c) TSE surface for combinations of three anti-cancer agents with concentrations C_1, C_2, and C_3. Exposure triples below the TSE surface (red) result in tumor growth, whereas exposure triples above the curve (green) result in tumor regression. (For interpretation of the references to color in this figure legend, the reader is referred to the web version of this article.)

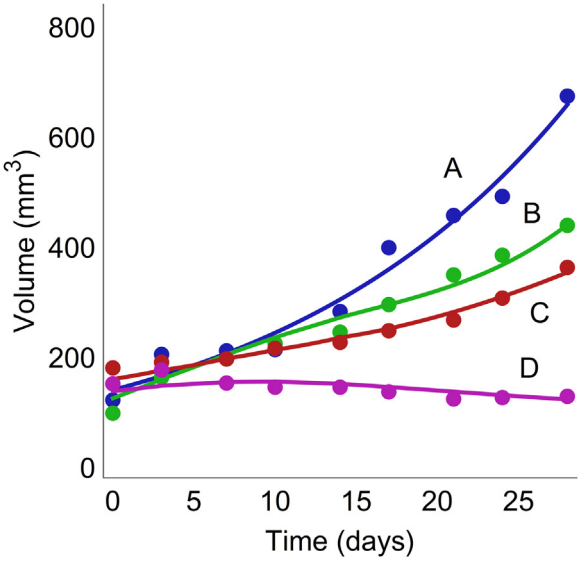

Fig. 2. Tumor volume (mm^3)-time courses of observed (symbols) and model-predicted (solid lines) data for each of the four treatment arms: (A) vehicle, (B) cetuximab monotherapy, (C) cisplatin monotherapy, and (D) combination therapy with cetuximab and cisplatin.

study were reported previously (Amendt et al., 2014; Cardilin et al., 2017). Experimental and model-predicted time courses for each of the four treatment arms are shown in Fig. 2.

3.3. Pharmacodynamic model analysis

Standard one- and two-compartment pharmacokinetic models were used to describe plasma exposure of cetuximab and cisplatin, respectively. The models, as well as the parameter estimates, were taken from the literature. Further details can be found in Cardilin et al. (2017).

A pharmacodynamic tumor model was developed to describe tumor evolution over time. The model consists of a main compartment of proliferating cells, and a set of damage compartments that each dying cell must traverse before disappearing. The drug action of cetuximab is described as an inhibition of the proliferation rate according to an inhibitory E_{max}-function ($I_{\max} = 1$), whereas the drug action of cisplatin is described as a linear stimulation of the natural death rate (Fig. 3).

The pharmacodynamic model is defined by the following system of differential equations

$$\begin{aligned}
\frac{dV_1}{dt} &= \left(1-\frac{C_{\text{cetuximab}}}{IC_{50}+C_{\text{cetuximab}}}\right)k_g V_1 - (1+bC_{\text{cisplatin}})k_k V_1 \\
\frac{dV_2}{dt} &= (1+bC_{\text{cisplatin}})k_k V_1 - k_k V_2 \\
\frac{dV_3}{dt} &= k_k V_2 - k_k V_3 \\
\frac{dV_4}{dt} &= k_k V_3 - k_k V_4 \\
V_{\text{total}} &= V_1 + V_2 + V_3 + V_4
\end{aligned} \tag{9}$$

where V_1 is the main compartment and V_2, V_3, and V_4 are the damage compartments, V_{total} is the total tumor volume, k_g and k_k are the growth and kill rates, IC_{50} is the concentration of cetuximab needed to achieve 50% inhibition of the proliferation, and b is a pharmacodynamic parameter associated with cisplatin. The initial conditions for each tumor volume compartment are given by

$$V_i(0) = \left(\frac{k_k}{k_g}\right)^{i-1} V^0, \quad i = 1, 2, 3, 4 \tag{10}$$

where V^0 is the initial volume of the main compartment. The parameter estimates for the TGI model were, as reported in the original article, $k_g = 0.0060\ \text{h}^{-1}$, $k_k = 0.0039\ \text{h}^{-1}$, $IC_{50} = 994\ \mu\text{g/mL}$, $b = 0.0093\ \text{mL/ng}$, and $V^0 = 60\ \text{mm}^3$.

3.4. Tumor static exposure for cetuximab and cisplatin

For the model in Eq. (9), an expression for the TSE curve can be found using the following reasoning: The main compartment, V_1, is the only compartment where cells proliferate. Hence, if V_1 is eradicated the entire tumor will eventually be eradicated as well. Therefore, if $dV_1/dt < 0$ the tumor will eventually be eradicated. Since V_1 will not be zero unless the tumor is already eradicated, this implies that Eq. (11) must hold.

$$\left(1-\frac{C_{\text{cetuximab}}}{IC_{50}+C_{\text{cetuximab}}}\right)k_g - (1+bC_{\text{cisplatin}})k_k < 0 \tag{11}$$

The TSE curve, which separates tumor growth from tumor shrinkage, will therefore consist of all concentration pairs ($C_{\text{cetuximab}}$, $C_{\text{cisplatin}}$) such that the left-hand side in Eq. (11) is equal to zero. Solving for $C_{\text{cisplatin}}$ gives

$$C_{\text{cisplatin}} = \frac{k_g}{bk_k}\left(1-\frac{I_{\max}C_{\text{cetuximab}}}{IC_{50}+C_{\text{cetuximab}}}\right) - \frac{1}{b} \tag{12}$$

Insertion of the pharmacodynamic parameter estimates for the tumor model into Eq. (12) produces the TSE curve shown in blue in Fig. 4. The region of concentration pairs that will lead to tumor eradication is shown in green, whereas the region that will not eradicate

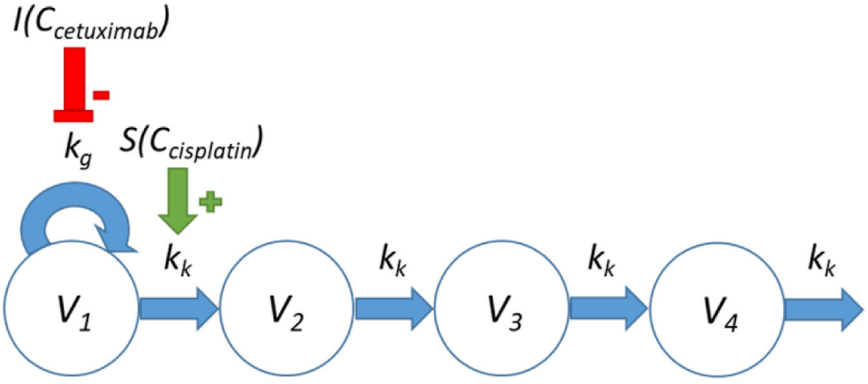

Fig. 3. Tumor growth inhibition TGI model for combination therapy with independent drug action. The model consists of a main compartment V_1 and three damage compartments, V_2, V_3, and V_4 that cells pass through before dying. Cetuximab (A) inhibits cell proliferation with inhibitory function $I(C_{\text{cetuximab}})$, whereas cisplatin (B) stimulates cell apoptosis with stimulatory function $S(C_{\text{cisplatin}})$. The k_g and k_k parameters represent the natural cell kill and death rates.

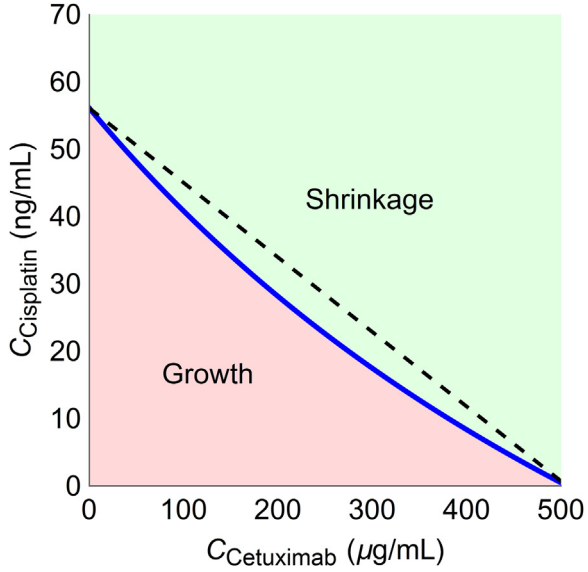

Fig. 4. The Tumor Static Concentration (TSE) curve for combinations of cetuximab and cisplatin plasma concentrations (blue, bold) separating regions of tumor growth (light red) and tumor shrinkage (light green). Reference straight line connecting the individual TSE values (black, dashed). (For interpretation of the references to color in this figure legend, the reader is referred to the web version of this article.)

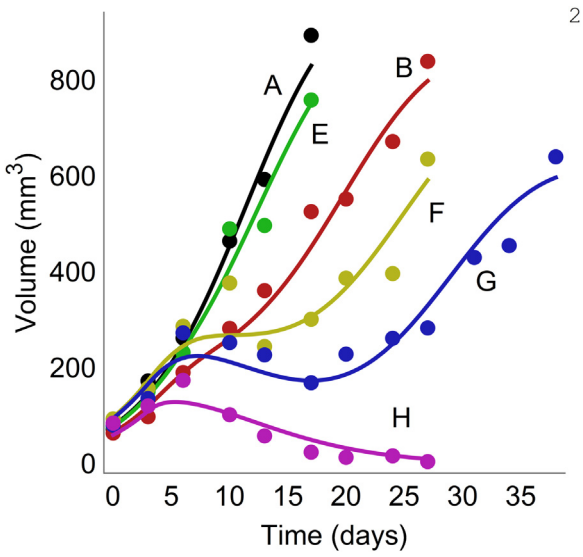

Fig. 5. Representative examples of individual fits for the following treatment arms: (A) vehicle, (B) radiation therapy with 2 Gy per dose, (E) RS1 monotherapy with 200 mg/kg per dose, and (F-H) combination therapy with 2 Gy per dose and 10, 50, or 200 mg/kg per dose of the radiosensitizer, respectively.

the tumor is shown in red. The intersections with the coordinate axes give the TSE values of 506 μg/mL and 56 ng/mL for cetuximab and cisplatin. These values correspond to the necessary exposure for tumor regression based on monotherapy with the respective compounds. The curve exhibits a weak curvature compared to a reference straight line between the TSE values (black, dashed).

The slight curvature indicates that there is only a slight advantage from combining the two compounds with respect to tumor regression. However, a complete assessment of the combination would also require taking into account the toxicity of both compounds when given as single agent as well as any toxicological interactions.

3.5. Translation of tumor static exposure to humans

Translation of the tumor model for cetuximab and cisplatin therapy and the associated TSE curve was considered by means of allometric scaling. The primary candidates for scaling were the rate constants k_g and k_k. Scaling is generally performed based on the relative body weight (BW) of the animals (mouse and man) with a typical value for the exponent of − 0.25 (West et al., 2002). Hence, the following parameter scalings were applied:

$$k_g^{\text{human}} = \left(\frac{BW^{\text{human}}}{BW^{\text{mouse}}}\right)^{-0.25} k_g^{\text{mouse}} \tag{13}$$

$$k_k^{\text{human}} = \left(\frac{BW^{\text{human}}}{BW^{\text{mouse}}}\right)^{-0.25} k_k^{\text{mouse}} \tag{14}$$

where typical body weights of human and mouse were assumed to be 70 kg and 25 g, respectively.

The TSE curve in Eq. (12) depends on the rate parameters only through their quotient, which will remain the same if the same scaling factor is used for k_g and k_k. Hence, from the perspective of allometric scaling, the TSE curve should be the same for mouse and human and Fig. 5 can be used for predictions in humans. Note, however, that realizations of the tumor model will look different depending on the allometric scaling used, but the qualitative behavior is the same (*i.e.*, growing or shrinking tumor).

3.6. Conclusions from case study I

The case study taught us to analyze tumor volume data obtained from different combinations of two different compounds, and how the TSE curve could be constructed and displayed. We did simulations of the time courses of tumor growth curves with different dose combinations of the two compounds. The resulting predictions showed the tumor volume-time behavior when we focused on chemical compound combinations targeting tumor shrinkage, tumor stasis or tumor growth. The TSE curve demonstrated a weak synergistic effect from combining cetuximab and cisplatin. An allometric scaling approach indicated that the predicted TSE curve may be the same across species.

4. Case study II: radiation and radiosensitizer

4.1. Problem formulation

This case study is based on results from a previous publication (Cardilin et al., 2018). Radiation therapy is commonly applied in cancer treatment for a wide range of tumors (Shaue and McBride, 2015). Radiation damages the DNA of cells, *e.g.*, through single- or double-strand breaks, and can lead to cell death or loss of the cell's proliferative capabilities (Eriksson and Stigbrand, 2010; Ross, 1999). The benefits of combining radiation therapy with different doses of a radiosensitizing agent were investigated. The goal was to develop a tumor model that describes experimental data of radiation and radiosensitizer treatment and to apply the model for evaluation of combinations with respect to synergy and overall efficacy using TSE curves. In addition, the translational aspects of the model were demonstrated for the human situation.

4.2. Experimental data

Eighty FaDu xenograft mouse models were used in the study. The mice were divided into eight treatment arms with $N = 10$ mice in each arm as follows: (A) vehicle, (B) radiation (2 Gy per dose), (C-E) monotherapy with a radiosensitizing compound (10, 50, or 200 mg/kg per dose), and (F-H) combination therapy (2 Gy and 10, 50, or 200 mg/kg per dose). Mice were given daily treatments for five days. Some tumor volume-time courses representing different treatment arms are

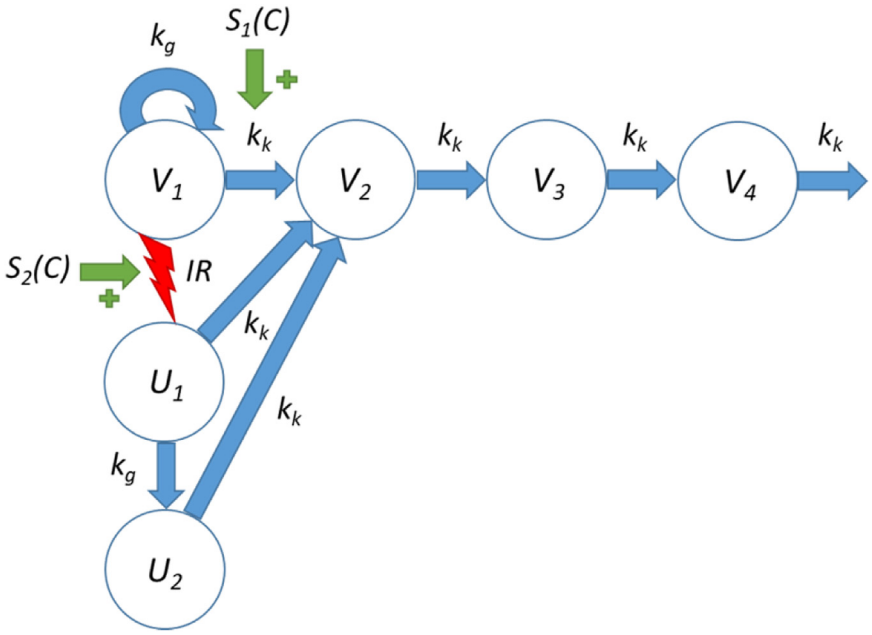

Fig. 6. Tumor model describing the radiation and radiosensitizing treatments. The vehicle model, shown in blue, consists of a main compartment V_1 of proliferating cancer cells with growth rate k_g and natural kill rate k_k. Before dying, cells must traverse a set of damage compartments V_2, V_3, and V_4. Radiation induces an instantaneous transfer of cells between V_1 and U_1, after which cells are allowed up to one more cell division before dying. The radiation-induced mass transfer is shown in red. The radiosensitizer stimulates both the natural death process (shown in green, $S_1(C)$) and the radiation-induced cell death (also shown in green, $S_2(C)$). The latter effect is only present in individuals treated with combination therapy. (For interpretation of the references to color in this figure legend, the reader is referred to the web version of this article.)

shown in Fig. 5. Further details of the study can be found in Cardilin et al. (2018).

4.3. Pharmacodynamic model analysis

Exposure to the radiosensitizing compound was described using a standard one-compartment model. To describe the tumor growth data, a TGI model was modified to account for radiation therapy. The modified model consists of a main compartment V_1 of proliferating cancer cells following logistic growth, and three damage compartments, V_2, V_3 and V_4, which cells must traverse before dying. Irradiated cells are instantaneously transferred to a separate compartment where they are allowed at most one more cell division before dying. Drug action of the radiosensitizing agent is described as separate stimulations of both the natural- and the radiation-induced cell deaths. The full model is shown in Fig. 6.

The tumor model was mathematically described using the following system of differential equations

$$\begin{aligned}
\frac{dV_1}{dt} &= k_g V_1\left(1-\frac{V_{\text{total}}}{K}\right) - S_1(C)k_k V_1 - (1-SF(D,C))RV_1 \\
\frac{dV_2}{dt} &= S_1(C)k_k V_1 + k_k U_1 + k_k U_2 - k_k V_2 \\
\frac{dV_3}{dt} &= k_k V_2 - k_k V_3 \\
\frac{dV_4}{dt} &= k_k V_3 - k_k V_4 \\
\frac{dU_1}{dt} &= (1-SF(D,C))RV_1 - k_g U_1 - k_k U_1 \\
\frac{dU_2}{dt} &= 2k_g U_1 - \quad k_k U_2 \\
V_{\text{total}} &= V_1 + V_2 + V_3 + V_4 + U_1 + U_2
\end{aligned} \tag{15}$$

where k_g is the growth rate, k_k the kill rate, K the tumor capacity parameter, R is the rate function for radiation, corresponding to a sequence of instantaneous cell transfers (mathematically described as a series of Dirac delta distributions), and S_1 is a linear stimulatory function of the radiosensitizer given by

$$S_1(C) = 1+aC \tag{16}$$

where a is a pharmacodynamic parameter associated with monotherapy with the radiosensitizer. The system in Eq. (15) has the initial conditions

$$V_i(0) = V^0\left(\frac{k_k}{k_g}\right)^{i-1}, \quad i = 1, 2, 3, 4 \quad \text{and } U_j(0) = 0, \quad j = 1, 2 \tag{17}$$

Finally, the fraction of lethally irradiated cells given a radiation dose D and concurrent plasma concentration C is given by

$$SF(D, C) = \exp[-S_2(C)(\alpha D + \beta D^2)], \quad \text{where } S_2(C) = 1+bC \tag{18}$$

where α and β are the linear and quadratic radiation parameters, respectively, and b is a pharmacodynamic parameter associated with stimulation of the radiation effect. Following a nonlinear-mixed effects approach, population parameter mean estimates were given by $k_g = 0.50\ \text{day}^{-1}$, $k_k = 0.28\ \text{day}^{-1}$, $K = 2200\ \text{mm}^3$, $V^0 = 40\ \text{mm}^3$, $\alpha = 0.08\ \text{Gy}^{-1}$, $\beta = 0.008\ \text{Gy}^{-2}$, $a = 0.09\ \text{mL}/\mu\text{g}$, and $b = 0.45\ \text{mL}/\mu\text{g}$.

4.4. Tumor Static Exposure (TSE) of radiation and radiosensitizer

The main compartment V_1 dominates the tumor model in the same sense as in Case study 1, *i.e.*, if V_1 is eradicated, the entire tumor will eventually be eradicated. In this case, cell proliferation is not exclusive to V_2, but is also included in the transfer from U_1 to U_2. However, the irradiated cells are only allowed to proliferate once (the resulting daughter cells are non-proliferating) and can therefore not sustain the tumor by themselves. Moreover, given that the treatment goal is tumor regression and ultimately eradication, we can safely ignore the saturation effect that occurs for large tumor volumes. The differential equation for V_1 in Eq. (15) therefore essentially reads

$$\frac{dV_1}{dt} = k_g V_1 - S_1(C)k_k V_1 - (1-SF(D,C))RV_1 \tag{19}$$

Upon irradiation at time $t = 0$, a fraction $SF(D, C(0))$ of the cells survive. This fraction will then continue to grow according to Eq. (19) until the time T of the next irradiation. The fraction of surviving cells, for times between the first and second instance of radiation, will be given by

$$V_1(t) = SF\left(D, C(0)\right)\exp\left(k_g t - k_k \int_0^t S_1(C(s))ds\right) \tag{20}$$

Hence, if $V_1(T) = V_1(0)$ the main compartment will be in approximate stasis, and if $V_1(T) < V_1(0)$ the main compartment will have shrunk. If such dosing is repeated, the main compartment will continue to shrink and eventually be eradicated. By using Eqs. (18) and (20), it is possible to derive an expression for the TSE curve (see Cardilin et al., 2018 for details). The main compartment will be in approximate stasis if

$$\left(1 + b\frac{\overline{C}k_e T}{1 - e^{-k_e T}}\right)(\alpha D + \beta D^2) - (k_g - k_k)T - k_k a T\overline{C} = 0 \tag{21}$$

where $\bar{C}$ is the average plasma concentration of the compound, and k_e is its elimination rate according to the pharmacokinetic model. The region of all average plasma concentrations and radiation doses that result in tumor shrinkage will therefore consist of those for which the left-hand side in Eq. (21) becomes negative. If we view Eq. (21) as a quadratic equation with respect to the radiation dose D we can use standard formulas to solve for D and find

$$D = \frac{-G(\alpha) + \sqrt{G(\alpha)^2 + 4G(\beta)(k_g T - k_k T - k_k a\overline{C})}}{2G(\beta)} \tag{22}$$

where D is the daily radiation dose, $\overline{C}$ denotes the average plasma concentration of the radiosensitizing compound over the period $[0, T]$, and the function G is given by

$$G(x) = x + \frac{b\overline{C}k_e Tx}{1 - e^{-k_e T}} \tag{23}$$

Inserting the population parameter values into Eq. (22) produces the TSE curve in Fig. 7. The curve exhibits a large curvature due to strong synergy between the treatments. In particular, the (relatively) large value of the interaction parameter b represents this synergy. The shrinkage, or eradication area (green) is therefore increased significantly compared to the case $b = 0$ (black, dashed curve). This means that tumor regression will be possible at much lower combination exposures.

In particular, we find the individual TSE values to be approximately 2.17 Gy for radiation and 8.26 μg/mL for the radiosensitizer, corresponding to monotherapy with either treatment.

4.5. Translation of tumor static exposure to humans

An allometric scaling approach was used to translate the tumor model and the associated TSE curve to humans (Boxenbaum, 1984; Kang and Lee, 2011). The rate constants k_g, k_k, and k_e, were scaled using a standard allometric exponent b = − 0.25 (Savage et al., 2008). Assuming body weights of 25 g and 70 kg for the mouse and man, respectively, the rate constants in man were decreased to approximately one seventh of their values in the mouse. Specifically, the rates were scaled as

$$k_g^{\text{human}} = \left(\frac{BW^{\text{human}}}{BW^{\text{mouse}}}\right)^{-0.25} k_g^{\text{mouse}} \tag{24}$$

$$k_k^{\text{human}} = \left(\frac{BW^{\text{human}}}{BW^{\text{mouse}}}\right)^{-0.25} k_k^{\text{mouse}} \tag{25}$$

$$k_e^{\text{human}} = \left(\frac{BW^{\text{human}}}{BW^{\text{mouse}}}\right)^{-0.25} k_e^{\text{mouse}} \tag{26}$$

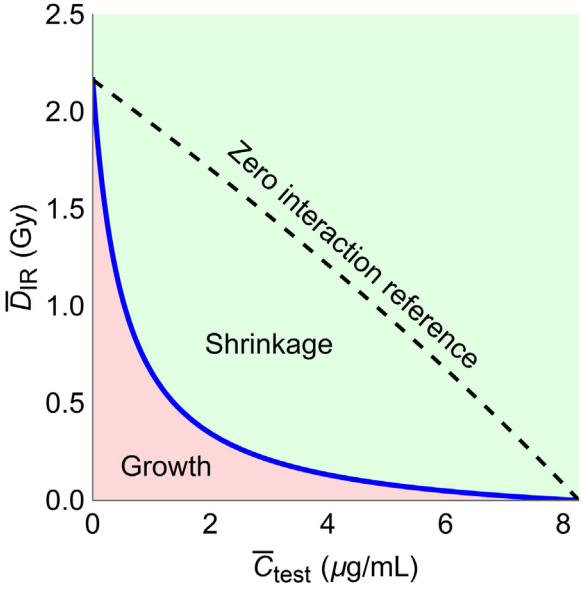

Fig. 7. The Tumor Static Exposure (TSE) curve as a function of radiation dose and radiosenzitizer concentration. The set of all concentration-dose pairs that yield tumor shrinkage upon daily administration is shown in green. Concentration pairs outside this region lead to tumor growth and are shown in red. The TSE curve is shown in blue and can be compared to the case with no synergy ($b = 0$), shown in black (dashed). The TSE curve has significant curvature due to a pronounced synergistic effect between the treatments. (For interpretation of the references to color in this figure legend, the reader is referred to the web version of this article.)

Moreover, the Dirac delta distribution, which describes the transfer of cells during irradiation, has a unit of 1/day and was therefore scaled in the same manner. Based on the allometrically scaled parameters, a prediction of TSE in man can be produced. Fig. 8 (left) shows the TSE curves for mouse (blue) and man (red), respectively. Fig. 8 (right) shows the resulting tumor growth curves following treatment with three different exposure levels (A, B, and C). Similarly to the TSC curve for cetuximab and cisplatin from case study I, the TSE values for monotherapy with either compound are the same for mouse and man. However, due to slower clearance in man, the corresponding TSE curve has less curvature. This follows because slower clearance makes the difference between peak and average plasma concentration smaller. Although the TSE curve exhibits less curvature, lower human clearance of the radiosensitizer suggests that less drug is needed to achieve a plasma concentration exceeding the TSE.

4.6. Conclusions from case study II

Case study II taught us to analyze tumor volume data obtained from different combinations of chemical and radiation interventions, and how the TSE curve was constructed and displayed for a relevant administration schedule. We also extended the underlying tumor model with a semi-mechanistic approach to show how intervention from chemicals and radiation jointly act upon the tissue growth/kill. The calibrated model showed good predictive capabilities for all treatment arms. The TSE curve associated with radiation and radiosensitizer combinations demonstrated a strong synergistic effect from combination therapy treatment. An allometric scaling approach showed differences in TSE across species due to differences in drug clearance.

5. Discussion

This paper was focused on two questions: Can quantitative techniques provide a better understanding of tumor volume data when combinations of chemicals and radiation are used? and What

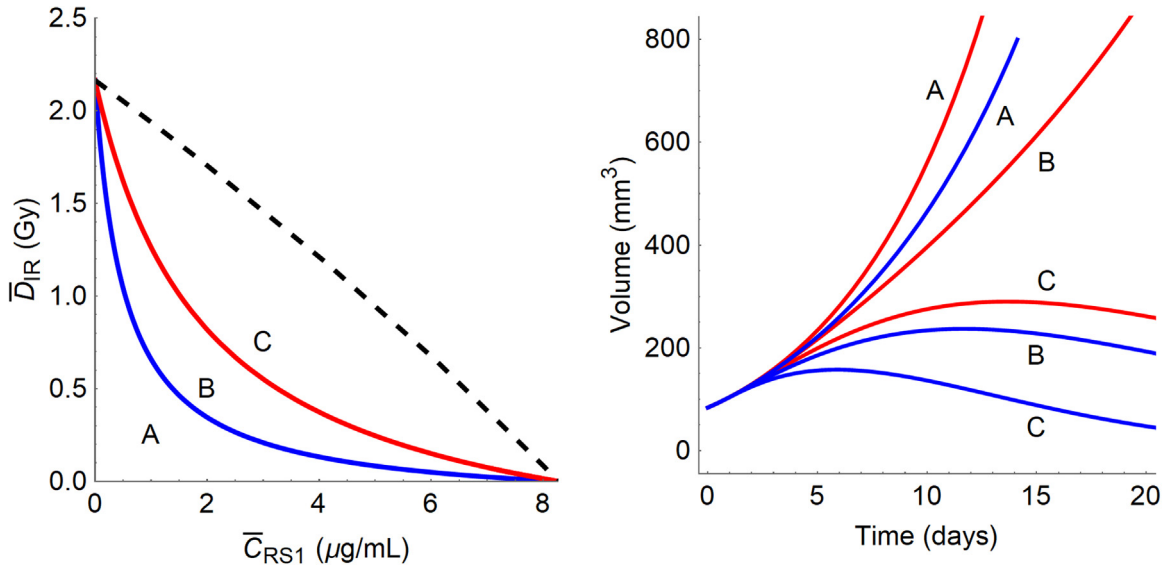

Fig. 8. (left) Predicted TSE curves for mouse (blue) and man (red), and (right) simulated tumor growth in mouse (blue) and man (red) following average exposures of A: (0.25 Gy, 1 μg/mL), B: (0.5Gy, 2 μg/mL), and C: (0.75Gy, 3 μg/mL). (For interpretation of the references to color in this figure legend, the reader is referred to the web version of this article.)

translational potential does such an approach have? We shall discuss these two questions in the rest of this section.

5.1. Quantitative tumor models

Quantitative techniques play an important role in modern pharmacology in order to improve our understanding of dose-exposure-response relationships (Standing, 2017; Gabrielsson and Green, 2009). In particular, pharmacokinetic and pharmacodynamic models have proven useful in describing tumor growth after administration of anticancer agents, displaying good predictive capabilities (Li et al., 2013; Zhu et al., 2015). In the case of combination therapy with multiple compounds, quantitative models have also been useful to identify and quantify potential drug synergies (Choo et al., 2013; Frances et al., 2011). We presented two models of combination therapies in oncology (Cardilin et al., 2017, 2018) and two case studies that involved combinations of two agents. Our results indicate that TSE can be used to assess and quantify synergy between different compounds, and that a quantitative approach provides a better understanding of tumor growth and how to intervene with combinations of drugs and/or therapies.

The first model, used to describe cetuximab and cisplatin, shares many similarities with previous tumor growth models (*e.g.*, Goteti et al., 2010; Rocchetti et al., 2013) but there are a few important differences. Firstly, our model incorporates a natural rate of cell death, meaning that even in the absence of treatment, some cells will be in the process of dying. This captures some of the heterogeneity of cancer cells and consequently provides a somewhat more biologically reasonable model. The inclusion of a natural death rate also meant that the initial distribution of cancer cells had to be revised (Cardilin et al., 2017).

The second model, used to describe radiation therapy combined with radiosensitizing treatment, has several novel aspects. One the one hand, the model can be seen as a generalization of the first model in that it includes the common structure of proliferating cells and a chain of transit compartments representing increasingly damaged cells (Simeoni et al., 2004). On the other hand, since we wanted to describe the effects of radiation therapy, we took some inspiration from the linear-quadratic theory of radiobiology (Brenner, 2008; Brenner et al., 1998). By combining these two perspectives, we arrived at a model that, while novel, is still founded on practical and empirical evidence. This was further consolidated when the model was used to predict the outcome following a prolonged administration schedule (Cardilin et al., 2018).

For both models we introduce the concept of TSE for combinations of anticancer agents. The TSE concept is a generalization of the Tumor Static Concentration value discussed by Jumbe et al. (2010) among others. TSE provides insight about drug efficacy and the *in* vivo sensitivity of tumor cells. In particular, TSE identifies drug exposure that is sufficient for tumor regression for monotherapies as well as combination therapies involving two or more compounds. Most importantly, TSE provides guidance for clinical dose regimen selection, where dosing interval troughs should exceed these concentrations for the effective tumor kill rate to exceed tumor growth rates for net antitumor activity. In other words, a quantitative approach provides a better understanding of tumor growth and how to intervene with combinations of drugs and/or therapies.

The two case studies we presented both involve combinations of two agents. The resulting TSE curves separate exposure pairs yielding tumor regression (green regions) from those that yield tumor growth (red regions). The curvature of the TSE curve is associated with the strength of synergy between the treatments. In case study I (cetuximab and cisplatin) the associated TSE curve (Fig. 4) indicated a weak synergistic effect, whereas in case study II (radiation and a radiosensitizer), the TSE curve (Fig. 7) indicated a strong synergy. We conclude that TSE can also be used to assess and quantify synergy between different compounds.

5.2. Translational potential

Since mechanism-based pharmacodynamic tumor models are based on measured exposure to drugs and complete volume-time curves, in contrast to the isobologram used for different dose combinations aiming at equal efficacies (Tallarida, 2006), the proposed concepts have a much stronger potential for translation of doses to systemic exposures, and observations in animal species to human plasma target concentrations. In an attempt to translate TSE to humans, we used an allometric scaling approach (Boxenbaum, 1982). We described how physiological or system parameters (*i.e.*, k_g and k_k) and drug rate parameters (k_e) may be allometrically scalable across different strains and species, including prediction of human doses. This approach is consistent with what has been tried for other tumor models (Herman et al., 2011; Lindauer et al., 2017). However, our approach relies on an assumption that drug-related parameters, *e.g.*, EC_{50}, are approximately the same across species. This is consistent with what others have

studied regarding allometric scaling of pharmacodynamic parameters (*e.g.,* Lui et al., 2016; Mager et al., 2009; Zuideveld et al., 2007). In particular, Mager et al. (2009) note that physiological turnover rates are often allometrically scalable across species, whereas parameters related to capacity and sensitivity tend to be similar. For the second model, we chose to scale the fraction lethally irradiated cells. One reason for this was reasonability – had we chosen not to scale this fraction, the necessary radiation doses tumor shrinkage would have been much lower than what is reasonable. Another argument is that the fraction of lethally irradiated tumor cells is formally described by a Dirac delta distribution with unit $days^{-1}$ and is therefore in a sense similar to a rate parameter. It is worth keeping in mind that allometry is not perfect and has not always agreed with empirical observations, and alternative approaches have been discussed, see for instance Agutter and Tuszynski (2011). When we applied allometric scaling to the model in case study I, the TSE curve remained the same across species. In contrast, when we applied allometric scaling to case study II, differences in drug clearance resulted in different curvatures of the TSE curves.

Finally, we believe that TSE is also applicable to different cell-lines since both growth (k_g) and natural cell kill (k_k) appear as intrinsic properties of the models. The models are not limited to a net growth expression, but instead consider separate growth and (natural) death rates. Moreover, the models encompass the utility of multiple drug (or radiation) interventions in their basic structure.

6. Conclusions

Our analysis focused specifically on deriving necessary mathematical tools and then implementing graphical ways to visualize additivity, synergy or antagonism based on exposure metrics. A quantitative mathematical/analytical approach strongly demonstrated its feasibility in pharmacology. The TSE analysis can easily be implemented in the drug discovery process and used as an independent approach to select or de-select compounds. The TSE concept has a unique potential for ranking of compounds and support the compound selection process in drug discovery, since it embodies model-based metrics of both drug (EC_{50}) and target properties (k_g and k_k), where all experimental data (tumor volume time courses) are taken into account. The graphical TSE method is a valuable way to communicate complicated processes to non-quantitative experts. The translational potential was shown in two case studies.

Acknowledgements

Tim Cardilin was supported by an education grant from Merck. This work was also partially funded by the Swedish Foundation for Strategic Research (Grant no. AM13-0046).

Appendix A

This appendix provides an introduction to the concepts of Tumor Static Concentration (TSC) and more generally, Tumor Static Exposure (TSE) from a mathematical perspective.

TSE for monotherapy with an anti-cancer agent

We consider a general tumor growth inhibition (TGI) model with n cell compartments with volumes $V_1, ..., V_n$ and exposure to an anti-cancer agent A

$$\frac{dV}{dt} = f(V;E), \qquad V(0) = V^0 \tag{A1}$$

where $V = (V_1, ..., V_n)$ is the vector of compartment volumes, $f = (f_1, ..., f_n)$ the growth rate of each compartment, $V^0 = (V_1^0, ..., V_n^0)$ is the vector of the initial volumes of each compartment at time $t = 0$, and E the exposure to compound A. Typically, we will have $E = C$, *i.e.*, the (plasma) concentration of the compound. However, in the case of radiation therapy for example, Dose-Response-Time modelling will need to be considered. Hence, $E = D$, the (radiation) dose. Theoretically, there could also be other ways of expressing the exposure to certain anti-cancer agents.

We shall first consider the case where E is constant and then move on to the case where E varies depending on the administration schedule. We would like to find all exposure levels of A that result in tumor eradication, *i.e.*, we are interested in the set

$$S = \left\{ E>0 : \lim_{t\to\infty} V(t;C) = 0, \quad \forall \quad V^0 \geq 0 \right\} \tag{A2}$$

If we further assume that anti-tumor activity is monotonically increasing with exposure, we are particularly interested in the smallest exposure that leads to tumor eradication, which we define as the *tumor static exposure* (TSE) value of compound A.

$$TSE_A = \inf_{E>0} S \tag{A3}$$

The TSE value will then have the property that for any $E>TSE_A$ the tumor will be eradicated following maintained exposure. When $E = C$ we shall sometimes also refer to the TSE value as the *tumor static concentration* (TSC). An illustration of the TSE value is given in Fig. 1a. The basic guideline would then be the following: choose an administration schedule for compound A such that the exposure level is kept above TSE_A. This will ensure tumor regression and eventual eradication.

TSE for combination therapy with two anti-cancer agents

For combination therapy with two compounds, denoted A_1 and A_2, we consider the same tumor model (Eq. (A1)) with exposure vector $E = (E_1, E_2)$, where E_1 represents the exposure to compound A_1 and E_2 represents the exposure to compound A_2. Analogously to the case with a single compound, we define the set S of simultaneous exposures E that yield tumor eradication

$$S = \left\{ (E_1, E_2)>0 : \lim_{t\to\infty} V(t;E) = 0, \quad \forall \quad V^0 \geq 0 \right\} \tag{A4}$$

The set S is a region in the positive exposure plane. We define the TSE *curve* to be the boundary of this set

$$TSE_{(A_1,A_2)} = \partial S \tag{A5}$$

The TSE curve divides the first quadrant of the exposure plane into two regions: one which will lead to tumor eradication, and another in which the tumor will persist. An illustration of a TSE curve is given in Fig. 1b. The points where the TSE curve intersects the coordinate axes will be the TSE values of the respective compounds. The general guideline remains the same: choose administration schedules for A_1 and A_2 such that the exposure pair E is kept above the TSE curve, *i.e.*, in the green region in Fig. 1b.

TSE for combination therapy with three or more anti-cancer agents

The TSE concept can be generalized to an arbitrary number of anti-cancer compounds, $A_1,..., A_m$ with an m-dimensional vector of exposures $E = (E_1,..., E_m)$. We define the set S

$$S = \left\{ E>0 : \lim_{t\to\infty} V(t;E) = 0, \quad \forall \quad V^0 \geq 0 \right\} \tag{A6}$$

and the TSE set as its boundary

$$TSE_{(A_1,...,A_m)} = \partial S \tag{A7}$$

In particular, for three compounds, the TSE set will be a surface in three-dimensional exposure space. An illustration of a TSE surface is given in Fig. 1c.

TSE for fixed administration schedules

An important generalization is to allow E to vary according to a given administration schedule. We shall consider administration schedules that are repeated. The simplest example being daily bolus dosing, but also, *e.g.*, biweekly dosing belongs to this category. The primary case is $E = D$, but another possibility would be to use the resulting average plasma concentration $\overline{C}$ when applicable. We can once more consider the tumor model in Eq. (A1), where we think of the administration schedule as being incorporated into f. We can now pose questions such as this: For which values of E, repeated according to the given administration, will the tumor eventually be eradicated? We then define the set S and the TSE value as in Eq. (A3). This construction can be performed for an arbitrary number of compounds in the same way as presented above.

Further generalizations of the TSE concept are possible. In particular, it is possible to consider different administration schedules. This means that E will be a time-varying function belonging to some vector space. The corresponding shrinkage set S will then consist of all, say L_2, functions E for which the tumor will be eradicated. Consequently, S will be a subset of an infinite-dimensional vector space of functions. This is the same perspective that is used in Optimal Control theory, which has been applied to different tumor models in order to optimize the treatment effect (Schättler and Ledzewics, 2015; Sbeity and Younes, 2015) However, because the optimal administration schedule is often difficult to determine, one has to settle for describing certain properties that the optimal solution possesses. Moreover, the solutions can be sensitive with respect to perturbations in the parameter estimates (Sbeity and Younes, 2015).

Declaration of interests

None.

References

Agutter, P.S., Tuszynski, J.A., 2011. Analytic theories of allometric scaling. J. Exp. Biol. 214, 1055–1062.

Amendt, C., Staub, E., Friese-Hamim, M., Störkel, S., Stroh, C., 2014. Association of EGFR expression level and cetuximab activity in patient-derived xenograft models of human non-small cell lung cancer. Clin. Cancer Res. 20 (17), 4478–4487. https://doi.org/10.1158/1078-0432.CCR-13-3385.

Baskar, R., Lee, K.A., Yeo, R., Yeoh, K.W., 2012. Cancer and radiation therapy: current advances and future directions. Int. J. Med. Sci. 9 (3), 193–199.

Bou-Assaly, W., Mukherji, S., 2010. Cetuximab (Erbitux). AJNR Am. J. Neuroradiol. 31 (4), 626–627.

Boxenbaum, H., 1982. Interspecies scaling, allometry, physiological time, and the ground plan of pharmacokinetics. J. Pharmacokinet. Biopharm. 10 (2), 201–227.

Boxenbaum, H., 1984. Interspecies pharmacokinetic scaling and the evolutionary-comparative paradigm. Drug Metab. Rev. 14 (5), 1071–1121.

Brenner, D.J., Hlatky, L.R., Hahnfeldt, P.J., Huang, Y., Sachs, R.K., 1998. The linear-quadratic model and most common radiobiological models result in similar predictions of time-dose relationships. Radiat. Res. 150 (1), 83–91.

Brenner, D.J., 2008. The linear-quadratic model is an appropriate methodology for determining iso-effective doses at large doses per fraction. Semin. Radiat. Oncol. 18 (4), 234–239. https://doi.org/10.1016/j.semradonc.2008.04.004.

Cardilin, T., Zimmermann, A., Jirstrand, M., Almquist, J., El Bawab, S., Gabrielsson, J., 2016. Extending the Tumor Static Concentration curve to average doses – a combination therapy example using radiation therapy. Page, Abstr 5975: ⟨www.page-meeting.org/?Abstract=5975⟩.

Cardilin, T., Almquist, J., Jirstrand, M., Sostelly, A., Amendt, C., El Bawab, S., Gabrielsson, J., 2017. Tumor static concentration curves in combination therapy. AAPS J. https://doi.org/10.1208/s12248-016-9991-1.

Cardilin, T., Almquist, J., Jirstrand, M., Zimmermann, A., El Bawab, S., Gabrielsson, J., 2018. Model-based evaluation of combination therapy in oncology. CPT: Pharmacomet. Syst. Pharmacol. 7 (1), 51–58. https://doi.org/10.1002/psp4.12268.

Choo, E.F., Ng, C.M., Berry, L., Belvin, M., Lewin-Koh, N., Merchant, M., Salphati, L., 2013. PK-PD modeling of combination efficacy effect from administration of the MEK inhibitor GDC-0973 and PI3K inhibitor GDC-0941 in A2058 xenografts. Cancer Chemother. Pharmacol. 71 (1), 133–143. https://doi.org/10.1007/s00280-012-1988-6.

Eriksson, D., Stigbrand, T., 2010. Radiation-induced cell death mechanisms. Tumour Biol. 31 (4), 363–372.

Evans, N.D., Dimelow, R.J., Yates, J.W., 2014. Modelling of tumour growth and cytotoxic effect of docetaxel in xenografts. Comput. Methods Prog. Biomed. 114 (3), e3–e13. https://doi.org/10.1016/ j.cmpb.2013.06.014.

Frances, N., Claret, L., Bruno, R., Iliadis, A., 2011. Tumor growth modeling from clinical trials reveals synergistic anticancer effect of the capecitabine and docetaxel combination in metastatic breast cancer. Cancer Chemother. Pharmacol. 68, 1413–1419.

Foucquier, J., Guedj, M., 2015. Analysis of drug combinations: current methodological landscape. Pharm. Res. Per. 3 (3), e00149. https://doi.org/10.1002/prp2.149.

Gabrielsson, J., Green, A.R., 2009. Quantitative pharmacology or pharmacokinetic pharmacodynamics integration should be a vital component in integrative pharmacology. J. Pharmacol. Exp. Ther. 331 (3), 767–774.

Gabrielsson, J., Gibbons, F.D., Peletier, L.A., 2016. Mixture dynamics: combination therapy in oncology. Eur. J. Pharm. Sci. 88, 132–146. https://doi.org/10.1016/j.ejps.2016.02.020.

Goteti, K., Garner, C.E., Utley, L., Dai, J., Ashwell, S., Moustakas, D.T., Gönen, M., Schwartz, G.K., Kern, S.E., Zabludoff, S., Brassil, P.J., 2010. Preclinical pharmacokinetic/pharmacodynamic models to predict synergistic effects of co-administered anti-cancer agents. Cancer Chemother. Pharmacol. 66 (2), 245–254. https://doi.org/10.1007/s00280-009-1153-z.

Grabovsky, Y., Tallarida, R.J., 2004. Isobolographic analysis for combinations of a full and partial agonist: curved isoboles. J. Pharm. Exp. Ther. 310 (3), 981–986.

Herman, A.B., Savage, V.M., West, G.B., 2011. A quantitative theory of solid tumor growth: metabolic rate and vascularization. PLoS One 6 (9), e22973.

Hutchinson, L.G., Mueller, H.-J., Gaffney, E.A., Maini, P.K., Wagg, J., Phipps, A., Boetsch,

C., Byrne, H.M., Ribba, B., 2016. Modeling longitudinal preclinical tumor size data to identify transient dynamics in tumor response to antiangiogenic drugs. CPT Pharmacomet. Syst. Pharmacol. 5 (11), 636–645. https://doi.org/10.1002/psp4.12142.

Jumbe, N.L., Xin, Y., Leipold, D.D., Crocker, L., Dugger, D., Mai, E., Sliwkowski, M.X., Fielder, P.J., Tibbitts, J., 2010. Modeling the efficacy of trastuzumab-DM1, an antibody drug conjugate, in mice. J. Pharmacokinet. Pharmacodyn. 37 (3), 221–242. https://doi.org/10.1007/s10928-010-9156-2.

Kang, H.E., Lee, M.G., 2011. Approaches for predicting human pharmacokinetics using interspecies pharmacokinetic scaling. Arch. Pharm. Res. 34 (11), 1779–1788.

Koch, G., Walz, A., Lahu, G., Schropp, J., 2009. Modeling of tumor growth and anticancer effects of combination therapy. J. Pharmacokinet. Pharmacodyn. 36 (2), 179–197. https://doi.org/10.1007/s10928-009-9117-9.

Koch, G., Schropp, J., Jusko, W.J., 2016. Assessment of non-linear combination effect terms for drug-drug interactions. J. Pharmacokinet. Pharmacodyn. 43 (5), 461–479. https://doi.org/10.1007/s10928-016-9490-0.

Li, M., Li, H., Cheng, X., Wang, X., Zhou, T., Lu, W., 2013. Preclinical pharmacokinetic/pharmacodynamic models to predict schedule-dependent interaction between erlotinib and gemcitabine. Pharm. Res. 30, 1400–1408.

Lindauer, A., Valiathan, C.R., Mehta, K., Sriram, V., de Greef, R., Elassaiass-Schaap, J., de Alwis, D.P., 2017. Translational pharmacokinetic/pharmacodynamic modeling of tumor growth inhibition supports dose-range selection of the Anti-PD-1 antibody pembrolizumab. CPT: Pharmacomet. Syst. Pharmacol. 6 (1), 11–20.

Lui, D., Ma, X., Liu, Y., Zhou, H., Shi, C., Wu, F., Jiang, J., Hu, P., 2016. Quantitative prediction of human pharmacokinetics and pharmacodynamics of imigliptin, a novel DPP-4 inhibitor, using allometric scaling, IVIVE and PK/PD modeling methods. Eur. J. Pharm. Sci. 89, 73–82.

Mager, D.E., Woo, S., Jusko, W.J., 2009. Scaling pharmacodynamics from in vitro and preclinical animal studies to humans. Drug Metab. Pharmacokinet. 24 (1), 16–24.

Magni, P., Simeoni, M., Poggesi, I., Rocchetti, M., De Nicolao, G., 2006. A mathematical model to study the effects of drugs administration on tumor growth dynamics. Math. Biosci. 200 (2), 127–151.

Miao, X., Koch, G., Straubinger, R.M., Jusko, W.J., 2016. Pharmacodynamic modeling of combined chemotherapeutic effects predicts synergistic activity of gemcitabine and trabectedin in pancreatic cancer cells. Cancer Chemother. Pharmacol. 77, 181–193. https://doi.org/10.1007/s00280-015-2907-4.

Mould, D.R., Walz, A.C., Lave, T., Gibbs, J.P., Frame, B., 2015. Developing exposure/response models for anticancer drug treatment: special considerations. CPT Pharmacomet. Syst. Pharmacol. 4 (1), e00016. https://doi.org/10.1002/psp4.16.

Reynolds, N.A., Wagstaff, A.J., 2004. Cetuximab: in the treatment of metastatic colorectal cancer. Drugs 64 (1), 109–118.

Ribba, B., Holford, N.H., Magni, P., Troconiz, I., Gueorguieva, I., Girard, P., Sarr, C., Elishmereni, M., Kloft, C., Friberg, L.E., 2014. A review of mixed-effects models of tumor growth and effects of anticancer drug treatment used in population analysis. CPT Pharmacomet. Syst. Pharmacol. 3, e113. https://doi.org/10.1038/psp.2014.12.

Rocchetti, M., Germani, M., Del Bene, F., Poggesi, I., Magni, P., Pesenti, E., De Nicolao, G., 2013. Predictive pharmacokinetic-pharmacodynamic modeling of tumor growth after administration of an anti-angiogenic agent, bevacizumab, as single-agent and combination therapy in tumor xenografts. Cancer Chemother. Pharmacol. 71 (5), 1147–1157. https://doi.org/10.1007/s00280-013-2107-z.

Ross, G.M., 1999. Induction of cell death by radiotherapy. Endocr. Relat. Cancer 6 (1), 41–44.

Savage, V.M., Deeds, E.J., Fontana, W., 2008. Sizing up allometric scaling. PLoS Comput. Biol. 4 (9), e1000171.

Sbeity, H., Younes, R., 2015. Review of optimization methods for cancer chemotherapy treatment planning. J. Comput. Sci. Syst. Biol. 8, 074–095. https://doi.org/10.4172/jcsb.1000173.

Schättler, H., Ledzewics, U., 2015. Optimal Control for Mathematical Models of Cancer Therapies. Springer, New York.

Shaue, D., McBride, W.H., 2015. Opportunities and challenges of radiotherapy for treating cancer. Nat. Rev. Clin. Oncol. 12 (9), 527–540.

Simeoni, M., Magni, P., Cammia, C., De Nicolao, G., Croci, V., Pesenti, E., Germani, M., Poggesi, I., Rocchetti, M., 2004. Predictive pharmacokinetic-pharmacodynamic modeling of tumor growth kinetics in xenograft models after administration of anticancer agents. Cancer Res. 64 (3), 1094–1101.

Standing, J.F., 2017. Understanding and applying pharmacometric modelling and simulation in clinical practice and research. Br. J. Clin. Pharmcol. 83 (2), 247–254.

Tallarida, R.J., 2006. An overview of drug combination analysis with isobolograms. J. Pharm. Exp. Ther. 319 (1), 1–7.

Tate, S.C., Cai, S., Ajamie, R.T., Burke, T., Beckmann, R.P., Chan, E.M., De Dios, A., Wishart, G.N., Gelbert, L.M., Cronier, D.M., 2014. Semi-mechanistic pharmacokinetic/pharmacodynamic modeling of antitumor activity of LY2835219, a new cyclin-dependent kinase 4/6 inhibitor, in mice bearing human tumor xenografts. Clin. Cancer Res. 20 (14), 3763–3774. https://doi.org/10.1158/1078-0432.CCR-13-2846.

Wendling, T., Mistry, H., Ogungbenro, K., Aarons, L., 2016. Predicting survival of pancreatic cancer patients treated with gemcitabine using longitudinal tumour size data. Cancer Chemother. Pharmacol. 77 (5), 927–938. https://doi.org/10.1007/s00280-016-2994-x.

West, G.B., Woodruff, W.H., Brown, J.H., 2002. Allometric scaling of metabolic rate from molecules and mitochondria to cells and mammals. Proc. Natl. Acad. Sci. USA 99 (Suppl. 1), S2473–S2478.

Zhu, X., Straubinger, R., Jusko, W.J., 2015. Mechanism-based mathematical modeling of combined gemcitabine and birinapant in pancreatic cancer cells. J. Pharmacokinet. Pharmacodyn. 42, 477–496.

Zuideveld, K.P., van der Graaf, P.H., Peletier, L.A., Danhof, M., 2007. Allometric scaling of pharmacodynamic responses: application to 5-Ht_{1A} receptor mediated responses from rat to man. Pharm. Res. 24 (11), 2031–2039.